Inorg. Chem. **2006**, *45*, 8365–8371

Dioxotungsten 1,2-Benzenedithiolate Complex Stabilized by NH···S Hydrogen Bonds

Koji Baba,[†] Taka-aki Okamura,*[,‡] Hitoshi Yamamoto,[‡] Tetsuo Yamamoto,[‡] Mitsuo Ohama,[‡] and Norikazu Ueyama*[,‡]

Chemical Analysis Research Center, National Institute for Agro-Environmental Sciences, Tsukuba, Ibaraki 305-8604, Japan, and Department of Macromolecular Science, Graduate School of Science, Osaka University, Toyonaka, Osaka 560-0043, Japan

Received April 28, 2006

Novel dioxo-tungsten(VI) bis(1,2-benzenedithiolate) complexes with neighboring amide groups, as models for tungsten enzymes, $(NEt_4)_2[W^{VI}O_2\{1,2\text{-}S_2\text{-}3,6\text{-}(RCONH)_2C_6H_2\}_2]$ (R = CH_3, *t*-Bu), were designed and synthesized. The presence of the NH···S hydrogen bond was confirmed through IR spectrometry and X-ray crystallographic analysis. In the $W^{VI}O_2$ complexes, the NH···S hydrogen bond trans to the oxo ligand is stronger than that cis to oxo. On the basis of comparisons with $[W^{VI}O_2(1,2\text{-}S_2C_6H_4)_2]^{2-}$, the NH···S hydrogen bond positively shifted the W(VI)/W(V) redox potentials and depressed the reduction by benzoin or triphenylphosphine. These results suggest that the NH···S hydrogen bond stabilizes the oxo ligand through trans influence and regulates O-atom transfer in tungsten and molybdenum enzymes.

Introduction

Tungsten enzymes are classified into two major groups: aldehyde oxidoreductases (AOR) and formate or *N*-formylmethanofuran dehydrogenases (F(M)DH) families. AORs can oxidize aliphatic and aromatic aldehyde to the corresponding carboxylic acids, whereas FDH can oxidize formate to carbon dioxide. Crystallographic and EXAFS studies have revealed the presence of an active tungsten site coordinated to two pyranopterin dithiolene moieties with a terminal oxo, hydroxo, or sulfido and an additional Ser, Cys, or Se•Cys ligand, which is analogous to the molybdenum enzymes.[1−7]

Many model complexes with various dithiolene (or pseudo-dithiolene) ligands and co-ligands have been synthesized and characterized.[8−13] Holm has investigated the reaction of tungsten enzyme models with biological or model substrates in considerable detail.[5,14−20] The electron-withdrawing substituents of the dithiolene ligand accelerated the oxo-transfer reaction to tungsten(IV) complexes.[15]

In our laboratory, the roles of the NH···S hydrogen bonds for a sulfur atom which is coordinated to a metal center in metalloenzymes have been studied using model com-

* To whom correspondence should be addressed. E-mail: tokamura@chem.sci.osaka-u.ac.jp (T.O.); ueyama@chem.sci.osaka-u.ac.jp (N.U.).
[†] National Institute for Agro-Environmental Sciences.
[‡] Osaka University.

(1) Chan, M. K.; Mukund, S.; Kletzin, A.; Adams, M. W.; Rees, D. C. *Science* **1995**, *267*, 1463−1469.
(2) Hu, Y. L.; Faham, S.; Roy, R.; Adams, M. W. W.; Rees, D. C. *J. Mol. Biol.* **1999**, *286*, 899−914.
(3) Raaijmakers, H.; Macieira, S.; Dias, J. M.; Teixeira, S.; Bursakov, S.; Huber, R.; Moura, J. J.; Moura, I.; Romao, M. J. *Structure* **2002**, *10*, 1261−1272.
(4) Hille, R. *Trends Biochem. Sci.* **2002**, *27*, 360−367.
(5) Musgrave, K. B.; Donahue, J. P.; Lorber, C.; Holm, R. H.; Hedman, B.; Hodgson, K. O. *J. Am. Chem. Soc.* **1999**, *121*, 10297−10307.
(6) Musgrave, K. B.; Lim, B. S.; Sung, K. M.; Holm, R. H.; Hedman, B.; Hodgson, K. O. *Inorg. Chem.* **2000**, *39*, 5238−5247.
(7) George, G. N.; Prince, R. C.; Mukund, S.; Adams, M. W. W. *J. Am. Chem. Soc.* **1992**, *114*, 3521−3523.
(8) Oku, H.; Ueyama, N.; Nakamura, A.; Kai, Y.; Kanehisa, N. *Chem. Lett.* **1994**, 607−610.
(9) Oku, H.; Ueyama, N.; Nakamura, A. *Inorg. Chem.* **1995**, *34*, 3667−3676.
(10) Das, S. K.; Biswas, D.; Maiti, R.; Sarkar, S. *J. Am. Chem. Soc.* **1996**, *118*, 1387−1397.
(11) Oku, H.; Ueyama, N.; Nakamura, A. *Chem. Lett.* **1996**, 31−32.
(12) Davies, E. S.; Aston, G. M.; Beddoes, R. L.; Collison, D.; Dinsmore, A.; Docrat, A.; Joule, J. A.; Wilson, C. R.; Garner, C. D. *J. Chem. Soc., Dalton Trans.* **1998**, 3647−3656.
(13) Eagle, A. A.; George, G. N.; Tiekink, E. R. T.; Young, C. G. *J. Inorg. Biochem.* **1999**, *76*, 39−45.
(14) Enemark, J. H.; Cooney, J. J.; Wang, J. J.; Holm, R. H. *Chem. Rev.* **2004**, *104*, 1175−1200.
(15) Sung, K. M.; Holm, R. H. *J. Am. Chem. Soc.* **2002**, *124*, 4312−4320.
(16) Sung, K. M.; Holm, R. H. *Inorg. Chem.* **2001**, *40*, 4518−4525.
(17) Sung, K. M.; Holm, R. H. *Inorg. Chem.* **2000**, *39*, 1275−1281.
(18) Miao, M. M.; Willer, M. W.; Holm, R. H. *Inorg. Chem.* **2000**, *39*, 2843−2849.
(19) Goddard, C. A.; Holm, R. H. *Inorg. Chem.* **1999**, *38*, 5389−5398.
(20) Tucci, G. C.; Donahue, J. P.; Holm, R. H. *Inorg. Chem.* **1998**, *37*, 1602−1608.

10.1021/ic060719t CCC: $33.50
Published on Web 09/09/2006

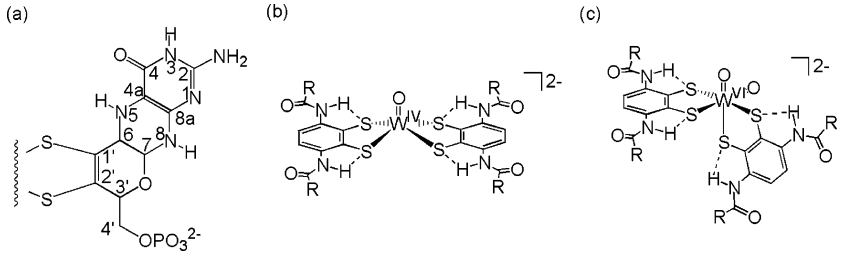

Figure 1. (a) Pterin 1,2-dithiolate. (b) $W^{IV}O$ model complex (R = CH_3, *t*-Bu). (c) $W^{VI}O_2$ model complex.

plexes.[21−27] It has been shown that NH···S hydrogen bonds positively shift the redox potentials, regulate the metal−sulfur bond strength, and protect the complexes from decomposition by air and moisture. In molybdenum enzyme model reactions, the acceleration of the reduction of Me_3NO was observed in the system of $[Mo^{IV}O(1,2\text{-}S_2C_2R_2)_2]^{2-}$ (R = CN, COOMe) and the multiamide additive ($(i\text{-}PrCONH)_2C_6H_4$),[28] which forms intermolecular NH···S hydrogen bonds. The NH···S hydrogen bonds between the sulfur atom of pterin dithiolene and amino acid residues are present in certain molybdenum enzymes.[29,30] For example, the dithiolene sulfur ligand interacts with Arg856 and Gln862 in the tungsten-containing formate dehydrogenase from *Desulfovibrio gigas*.[3] Additionally, in pterin dithiolene, the N···S distances between N5 nitrogen and dithiolene sulfur are notably short (3.07−3.61 Å) (Figure 1),[1−3] which suggests the presence of NH···S hydrogen bonds. Recently, we have synthesized novel $Mo^{IV}O$ 1,2-benzenedithiolate complexes with intraligand NH···S hydrogen bonds as models for molybdenum enzymes and found accelerated reduction of Me_3NO by NH···S hydrogen bonds.[31] But we could not isolate the resulting $Mo^{VI}O_2$ 1,2-benzenedithiolate complexes because of their instability. This instability is probably caused by the positive shift of the Mo(V/VI) redox potential. The molybdenum(VI) complexes were reductively decomposed to the molybdenum(IV) complex via reactive $Mo^{V}O_2$ species (not detected) accompanying oxidation of the ligands. Therefore, the role of NH···S hydrogen bonds in the oxidized state could not be investigated. Because the tungsten complex exhibits more negative redox potential than the corresponding molybdenum one, the dioxotungsten(VI) dithiolate complex should be thermodynamically more stable and show lower reactivity to reducing substrates than the molybdenum(VI) analogue.[32] This trend is known as the "metal effect".[33] Tungsten DMSO reductase exhibits negative redox potential, showing no ability to catalyze the oxidation of DMS (dimethyl sulfide) to DMSO, while the reduction of DMSO is faster than with the native DMSO reductase.[34]

In this paper, we describe the synthesis, structure, and reactivity of monooxotungsten(IV) and dioxotungsten(VI) 1,2-benzenedithiolate complexes with intramolecular NH···S hydrogen bonds (Figure 1). This work augments our previous studies of the corresponding molybdenum model system.[31]

Experimental Section

Materials. All procedures were carried out under an argon atmosphere. *N*,*N*-Dimethylacetamide, triethylamine, *N*,*N*-dimethylformamide (DMF), methanol, and acetonitrile were purified by distillation before use. Other reagents were obtained commercially and used without further purification. Ligand precursors, $\{1,2\text{-}S_2\text{-}3,6\text{-}(RCONH)_2C_6H_2\}_2$ (R = CH_3 (**1**), *t*-Bu (**2**)), were synthesized by the method described in our previous report.[31]

$(NEt_4)_2[W^{IV}O\{1,2\text{-}S_2\text{-}3,6\text{-}(CH_3CONH)_2C_6H_2\}_2]$ (3). An acetonitrile (5 mL) solution of $\{1,2\text{-}S_2\text{-}3,6\text{-}(CH_3CONH)_2C_6H_2\}_2$ (209 mg, 0.41 mmol) and tetraethylammonium borohydride (200 mg, 1.38 mmol) was added to a solution of $(NEt_4)[W^{V}O(SPh)_4]$[35] (314 mg, 0.41 mmol) in a mixture of acetonitrile (20 mL) and water (2 mL). The mixture was stirred overnight, and then the solution was reduced to dryness. The residue was dissolved in acetonitrile (12 mL), and the insoluble materials were removed by filtration. The filtrate was reduced to a volume of 2 mL, and diethyl ether (10 mL) was added dropwise to precipitate a yellow powder, which was recrystallized from acetonirile/diethyl ether to give yellow mirocrystals. For the X-ray structure, crystals were grown from DMF/diethyl ether. Yield: 350 mg (88%). Anal. Calcd for $C_{68}H_{60}N_6O_5WS_4\cdot(MeCN)_2\cdot(Et_2O)_2$: C, 48.07; H, 7.23; N, 9.34. Found: C, 48.18; H, 7.35; N, 8.90. ^{1}H NMR (DMSO-d_6, anion): δ 9.00 (s, 4), 7.62 (s, 4), 2.19 (s, 12). The microcrystals of **3**−**5** contained solvents that were detected by ^{1}H NMR spectra.

$(NEt_4)_2[W^{IV}O\{1,2\text{-}S_2\text{-}3,6\text{-}(t\text{-}BuCONH)_2C_6H_2\}_2]$ (4). This complex was prepared with a similar procedure from a solution of $(NEt_4)[W^{V}O(SPh)_4]$ (300 mg, 0.39 mmol), $\{1,2\text{-}S_2\text{-}3,6\text{-}(t\text{-}BuCONH)_2C_6H_2\}_2$ (269 mg, 0.40 mmol), and tetraethylammonium

(21) Okamura, T.; Ueyama, N.; Nakamura, A.; Ainscough, E. W.; Brodie, A. M.; Waters, J. M. *J. Chem. Soc., Chem. Commun*. **1993**, 1658−1660.
(22) Okamura, T.; Takamizawa, S.; Ueyama, N.; Nakamura, A. *Inorg. Chem.* **1998**, *37*, 18−28.
(23) Ueyama, N.; Nishikawa, N.; Yamada, Y.; Okamura, T.; Nakamura, A. *J. Am. Chem. Soc.* **1996**, *118*, 12826−12827.
(24) Ueyama, N.; Okamura, T.; Nakamura, A. *J. Chem. Soc., Chem. Commun.* **1992**, 1019−1020.
(25) Ueyama, N.; Okamura, T.; Nakamura, A. *J. Am. Chem. Soc.* **1992**, *114*, 8129−8137.
(26) Ueyama, N.; Taniuchi, K.; Okamura, T.; Nakamura, A.; Maeda, H.; Emura, S. *Inorg. Chem.* **1996**, *35*, 1945−1951.
(27) Ueyama, N.; Yamada, Y.; Okamura, T.; Kimura, S.; Nakamura, A. *Inorg. Chem.* **1996**, *35*, 6473−6484.
(28) Oku, H.; Ueyama, N.; Nakamura, A. *Inorg. Chem.* **1997**, *36*, 1504−1516.
(29) Dias, J.; Than, M.; Humm, A.; Bourenkov, G. P.; Bartunik, H. D.; Bursakov, S.; Calvete, J.; Caldeira, J.; Carneiro, C.; Moura, J. J.; Moura, I.; Romao, M. J. *Structure* **1999**, *7*, 65−79.
(30) Boyington, J. C.; Gladyshev, V. N.; Khangulov, S. V.; Stadtman, T. C.; Sun, P. D. *Science* **1997**, *275*, 1305−1308.
(31) Baba, K.; Okamura, T.; Suzuki, C.; Yamamoto, H.; Yamamoto, T.; Ohama, M.; Ueyama, N. *Inorg. Chem.* **2006**, *45*, 894−901.
(32) Ueyama, N.; Oku, H.; Nakamura, A. *J. Am. Chem. Soc.* **1992**, *114*, 7310−7311.
(33) Sung, K. M.; Holm, R. H. *J. Am. Chem. Soc.* **2001**, *123*, 1931−1943.
(34) Hagedoorn, P.-L.; Hagen, W. R.; Stewart, L. J.; Docrat, A.; Bailey, S.; Garner, C. D. *FEBS Lett.* **2003**, *555*, 606−610.
(35) Hanson, G. R.; Brunette, A. A.; McDonell, A. C.; Murra, K. S.; Wedd, A. G. *J. Am. Chem. Soc.* **1981**, *103*, 1953−1959.

borohydride (179 mg, 1.24 mmol) in acetonitrile (20 mL) and water (2 mL). Yield: 330 mg (74%). Anal. Calcd for $C_{48}H_{84}N_6O_5WS_4 \cdot (MeCN) \cdot (Et_2O) \cdot (H_2O)_2$: C, 50.33; H, 7.91; N, 7.61. Found: C, 50.19; H, 8.01; N, 7.90. ^{1}H NMR (DMSO-d_6, anion): δ 8.96 (s, 4), 7.60 (s, 4), 1.19 (s, 36). The hygroscopic character of **4** and **6** resulted in the taking up of moisture during sampling for the elemental analysis.

$(NEt_4)_2[W^{VI}O_2\{1,2\text{-}S_2\text{-}3,6\text{-}(CH_3CONH)_2C_6H_2\}_2]$ (5). A solution of Me_3NO (100 mM) in DMF (1.03 mL) was added to a solution of **3** (100 mg, 0.103 mmol) in DMF (10 mL). The solution immediately turned red. After 10 min, the solution was evaporated to dryness and then recrystallized from methanol. Yield: 90 mg (86%). Anal. Calcd for $C_{68}H_{60}N_6O_6WS_4 \cdot CH_3OH$: C, 43.70; H, 6.34; N, 8.26. Found: C, 43.51; H, 6.53; N, 8.24. ^{1}H NMR (DMSO-d_6, anion): δ 8.46 (s, 4), 7.31 (s, 4), 2.03 (s, 12).

$(NEt_4)_2[W^{VI}O_2\{1,2\text{-}S_2\text{-}3,6\text{-}(t\text{-}BuCONH)_2C_6H_2\}_2]$ (6). A solution of Me_3NO (100 mM) in DMF (0.88 mL) was added to a solution of **4** (100 mg, 0.088 mmol) in DMF (10 mL). The solution gradually turned red. After 60 min, the solution was reduced to a volume of 1 mL, and diethyl ether (5 mL) was added dropwise to precipitate a red powder. Yield: 80 mg (79%). Anal. Calcd for $C_{48}H_{84}N_6O_6WS_4 \cdot (H_2O)_2$: C, 48.47; H, 7.46; N, 7.07 Found: C, 48.20; H, 7.74; N, 7.10. ^{1}H NMR (DMSO-d_6, anion): δ 8.46 (s, 4), 7.33 (s, 4), 1.19 (s, 36).

Physical Measurements. UV−vis absorption spectra were recorded using a SHIMADZU UV-3100 and UV-3150 PC spectrophotometer (M^{-1} cm^{-1}). IR spectroscopic measurement in the solid state was done on a Jasco FT/IR-8300 spectrometer. Samples were prepared as KBr pellets. ^{1}H NMR spectra were obtained with a JEOL GSX-400 and ALPHA-600 in acetonitrile-d_3 or dimethyl sulfoxide-d_6 at 27 °C. The measurements of cyclic voltammograms in DMF solution were carried out on a BAS 100B/W instrument with a three-electrode system: glassy carbon working electrode, a Pt-wire auxiliary electrode, and saturated calomel electrode (SCE). The scan rate was 0.1 V/s, if not described. The concentration of sample was 1 mM, containing 0.1 M of *n*-Bu_4NClO_4 as a supporting electrolyte. Potentials were determined at room temperature versus SCE as a reference. All results were cross-referenced using the ferrocene/ferrocenium couple as a calibrant. The Raman spectra were measured at 298 K on a Jasco NR-1800 spectrophotometer. Exciting radiation was provided by Ar^+ ion (514.5 nm), if not described. The acetonitrile solution of each sample was added into a glass ampule and dried slowly in vacuo to form a thin layer.

Kinetic Measurements. Reaction solutions containing the monooxotungsten(IV) complex and Me_3NO systems were monitored spectrophotometrically. A typical measurement was carried out using a 10 mm UV cell containing a solution of monooxotungsten(IV) complex (0.1 mM) in DMF at 27 °C. After thermal equilibrium, a Me_3NO solution (~100 mM in DMF) was injected through glass stopcock, and the contents were quickly mixed by shaking. The time-dependent change in the concentration of the dioxotungsten(VI) complex was monitored at 323 nm for **3** and 385 nm for **4** every 5 s.

The reaction solution containing the dioxotungsten(VI) complex and the Ph_3P system was monitored using an NMR spectrometer. A solution of Ph_3P (100 mM) in acetonitrile-d_3 (0.060 mL) was added to a solution of dioxotungsten(VI) complex (1 mM) in acetonitrile-d_3 (0.60 mL) at 27 °C. The reaction proceeded stoichiometrically and was analyzed using the ratio of the amide proton signals of **5** (8.74 ppm) and **3** (8.23 ppm).

X-ray Structure and Determination. Single crystals of **3**·2DMF and **5**·CH_3OH were sealed in individual glass capillaries under an argon atmosphere for the X-ray measurements. X-ray measurements were performed on a Rigaku AFC5R diffractometer for **3**·2DMF and a Rigaku RAXIS−RAPID imaging plate for **5**·CH_3OH. The radiation used was Mo Kα, monochromatized with graphite (0.7107 Å). Crystallographic data are summarized in Table 1. All of the calculations were carried out using the teXsan crystallographic software package of the Molecular Structure Corp. The structures were solved by a direct method with SHELXS-97[36] for **3**·2DMF and SIR92[37] for **5**·CH_3OH, expanded using Fourier techniques, and refined by a full-matrix least-squares method anisotropically for non-hydrogen atoms using SHELXL-97.[38] All hydrogen atoms were generated geometrically. Atom scattering factors and dispersion corrections were taken from the International Tables.[39] For **3**·2DMF, the position of W═O was found to be disordered resulting in poor accuracy in the bond length.

Table 1. Crystallographic Data

	3·2DMF	**5**·CH_3OH
formula	$C_{42}H_{74}N_8O_7S_4W$	$C_{37}H_{64}N_6O_7S_4W$
fw	1115.18	1017.03
cryst syst	monoclinic	monoclinic
space group	*C*2/*c*	*C*2/*c*
T (K)	296	200
a (Å)	21.371(4)	19.75(3)
b (Å)	9.099(5)	20.38(3)
c (Å)	28.513(3)	13.06(2)
β (deg)	108.854(11)	118.24(5)
V (Å^3)	5247(3)	4632(13)
Z	4	4
d_{calcd} (g/cm^3)	1.412	1.458
μ (mm^{-1})	2.412	2.723
GOF (F^2)	1.000	1.000
R1[a] [$I > 2\sigma(I)$]	0.0670	0.0442
wR2[b] (all data)	0.1665	0.0858

[a] $R1 = \sum||F_o| - |F_c||/\sum|F_o|$. [b] $wR2 = \{\sum[w(F_o^2 - F_c^2)^2]/\sum[w(F_o^2)^2]\}^{1/2}$.

Results and Discussion

Synthesis. Monooxotungsten(IV) complexes **3** and **4** were prepared by a ligand-exchange reaction of $(NEt_4)[W^VO(SPh)_4]$ with **1** or **2** in the presence of tetraethylammonium borohydride in a mixture of acetonitrile and water. A similar method was previously employed for the synthesis of the corresponding molybdenum complexes.[31] When the reaction was performed without water, a tris(1,2-benzenedithiolate) complex, $(NEt_4)_2[W^{IV}\{1,2\text{-}S_2\text{-}3,6\text{-}(RCONH)_2C_6H_2\}_3]$, was isolated in a high yield. The monooxotungsten(IV) complexes readily react with trimethylamine *N*-oxide in acetonitrile solution to give the corresponding dioxotungsten(VI) complexes **5** and **6**. The dioxotungsten(VI) complexes were successfully isolated, different from the unstable dioxomolybdenum(VI) complexes.

Crystal Structures. The crystal structures of **3**·2DMF and **5**·CH_3OH are shown in Figure 2. The crystal structure of **3**·2DMF was disordered; therefore, the bond lengths and angles will not be discussed in detail. The other minor

(36) Sheldrick, G. M. *SHELXS-97*; University of Göttingen: Göttingen, Germany, 1997.
(37) Altomare, A.; Cascaano, G.; Giacovazzo, C.; Guagliardi, A.; Burla, M. C.; Polidori, G.; Camalli, M. *J. Appl. Crystallogr*. **1994**, *27*, 435−450.
(38) Sheldrick, G. M. *SHELXL-97*; University of Göttingen: Göttingen, Germany, 1997.
(39) Cromer, D. T.; Waber, J. T. *International Tables for X-ray Crystallography*; Kynoch Press: Birmingham, U. K., 1974; Vol. IV.

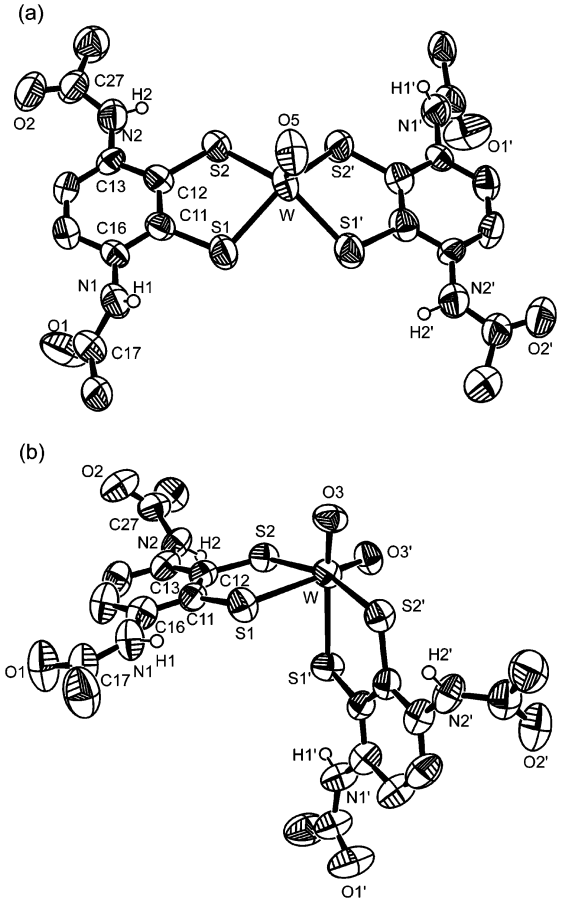

Figure 2. ORTEP drawings: (a) **3**·2DMF (anion part) and (b) **5**·CH_3OH (anion part).

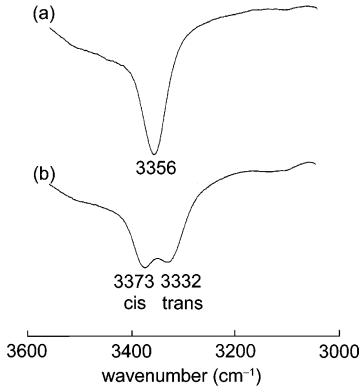

Figure 3. IR spectra of (a) **4** and (b) **6** (KBr disk) in the NH region: cis and trans represent the positions from the oxo ligands.

W═O moiety (W1B═O5B) was found at the opposite site of S_4 plane along the major W═O (W1A═O5A) bond. Two W═O groups are in a pseudo-centrosymmetry including the dithiolato ligands (please see Supporting Information). This linear O5═W1A−W1B═O5B arrangement resulted inaccurate positions of these atoms. A similar situation was found in the molybdenum analogue.[32] The W centers of **3**·2DMF and **5**·CH_3OH show a square pyramidal and a distorted octahedral geometry similar to those of $(NEt_4)_2[W^{IV}O(bdt)_2]$ (**7**)[24] and $(PPh_4)_2[W^{VI}O_2(bdt)_2]$ (**8a**),[40] respectively. The

(40) Ueyama, N.; Oku, H.; Nakamura, A. *J. Am. Chem. Soc.* **1992**, *114*, 7310−7311.

Table 2. Selected Bond Distances (Å) and Angles (deg)

	5·CH_3OH	**8a**[a]
mean W═O	1.735(4)	1.730(7)
mean W−S (trans to oxo)	2.607(3)	2.597(10)
mean W−S (cis to oxo)	2.426(4)	2.425(12)
mean S−C (trans to oxo)	1.757(5)	1.751(7)
mean S−C (cis to oxo)	1.752(5)	1.740(4)
mean W−S−C (trans to oxo)	106.6(2)	106.3(2)
mean W−S−C (cis to oxo)	111.24(19)	110.4(0)
S1···N1	2.964(6)	
S2···N2	2.944(6)	
C17−N1−C16−C15	7.9(9)	
C27−N2−C13−C14	49.7 (8)	

[a] Ref 37.

Table 3. IR Bands of ν(NH) and ν(C═O)

	W complex[a]	$(S\text{-}2\text{-}RCONHC_6H_4)_2$[b]	$\Delta\nu$(NH)	ν(C═O)
		$W^{IV}O$		
3	3346	3382	−36	1670
4	3356	3397	−41	1677
		$W^{VI}O_2$		
5	3370, 3316	3382	−12, −66	1672
6	3373, 3332	3397	−24, −65	1677

[a] KBr pellet. [b] In CH_2Cl_2 (10 mmol L^{-1}).

structural data of **5**·CH_3OH are compared to those of **8a** in Table 2. Both the W atoms were found at the special position on the crystallographic C_2 axis. The W═O3, W−S1 (trans to oxo), and W−S2 (cis to oxo) bond lengths of **5** are statistically equivalent to those of **8a**. The trans influence (longer W−S1 bond than W−S2) was also observed.[41] The short intraligand N1···S1 (2.96 Å) and the coplanarity between the amide plane and the benzene ring (C17−N1−C16−C15 = 7.9°) suggest the presence of an N1H···S1 hydrogen bond. On the other hand, the larger C27−N2−C13−C14 torsion angle (49.7°) is not so favorable to form N2H···S2 hydrogen bond. These data suggest the NH···S hydrogen bonds at the trans position to the oxo ligand are stronger then those at the cis position. In a solution, these NH protons were not distinguished by ^1H NMR. Two amide groups are probably exchanged rapidly in the time scale of NMR spectroscopy by a cis−trans isomerization in octahedral geometry via a trigonal prismatic intermediate. The interatomic distance between the sulfur (S1) atom and the amide proton (H1) is 2.45 Å, which is shorter than that between S2 and H2 by 0.28 Å.

IR and Raman Spectra. The NH stretching bands of **4** and **6** in the solid state are shown in Figure 3. The ν(NH) and ν(C═O) bands of **3**−**6** are summarized in Table 3 with the NH stretches of the free disulfide, $(S\text{-}2\text{-}RCONHC_6H_4)_2$ (R = CH_3, *t*-Bu),[42] in CH_2Cl_2 solution (10 mM). These disulfides were used as references because both **1** and **2** are insoluble in a less polar organic solvent such as CH_2Cl_2 or CH_3CN. The Δ(NH) indicates the difference from the ν-(NH) of the free disulfide.

(41) Ueyama, N.; Oku, H.; Kondo, M.; Okamura, T.; Yoshinaga, N.; Nakamura, A. *Inorg. Chem.* **1996**, *35*, 643−650.
(42) Ueyama, N.; Nishikawa, N.; Yamada, Y.; Okamura, T.; Oka, S.; Sakurai, H.; Nakamura, A. *Inorg. Chem.* **1998**, *37*, 2415−2421.

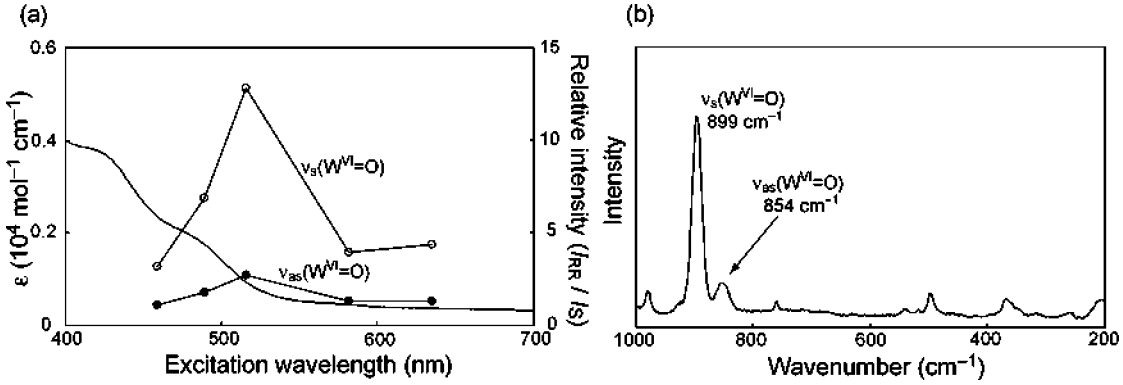

Figure 4. (a) Raman excitation profile and (b) Raman spectra of **5**.

Table 4. Raman and IR Bands in the Solid State

	IR band (ν(W^{IV}=O))
W^{IV}O	
$(NEt_4)_2[W^{IV}O\{1,2\text{-}S_2\text{-}3,6\text{-}(CH_3CONH)_2C_6H_2\}_2]$ (**3**)	912
$(NEt_4)_2[W^{IV}O\{1,2\text{-}S_2\text{-}3,6\text{-}(t\text{-}BuCONH)_2C_6H_2\}_2]$ (**4**)	925
$(NEt_4)_2[W^{IV}O(bdt)_2]$ (**7**)[a]	906
$(NEt_4)_2[W^{IV}O\{1,2\text{-}S_2C_2(CN)_2\}_2]$[b]	935
$(NEt_4)_2[W^{IV}O\{1,2\text{-}S_2C_2(CH_3)_2\}_2]$[c]	897

	Raman band ν_s(W^{VI}=O) ν_{as}(W^{VI}=O)	IR band ν_s(W^{VI}=O) ν_{as}(W^{VI}=O)
W^{VI}O$_2$		
$(NEt_4)_2[W^{VI}O_2\{1,2\text{-}S_2\text{-}3,6\text{-}(CH_3CONH)_2C_6H_2\}_2]$ (**5**)	899, 854	893, 847
$(NEt_4)_2[W^{VI}O_2\{1,2\text{-}S_2\text{-}3,6\text{-}(t\text{-}BuCONH)_2C_6H_2\}_2]$ (**6**)	903, 857	899, 855
$(NEt_4)_2[W^{VI}O_2(bdt)_2]$ (**8b**)[a]	885, 843	888, 847
$(NEt_4)_2[W^{VI}O_2\{1,2\text{-}S_2C_2(CN)_2\}_2]$[b]		906, 860
$(NEt_4)_2[W^{VI}O_2\{1,2\text{-}S_2C_2(CH_3)_2\}_2]$[c]		876, 833

[a] Ref 43. [b] Ref 10. [c] Ref 19.

The tungsten(VI) complex **6** exhibited two ν(NH) bands at 3373 and 3332 cm^{-1}, whereas tungsten(IV) complex **4** indicated a single band at 3356 cm^{-1}. A similar trend was observed for **3** and **5**. The two bands are attributed to two kinds of NH groups at the cis and trans positions. The larger negative shifts, -66 cm^{-1} for **5** and -65 cm^{-1} for **6**, are attributed to the stronger NH···S hydrogen bond at the trans position to oxo ligand as suggested in the crystal structure. The strong NH···S hydrogen bond probably stabilizes the negative charge on sulfur atom which is accumulated by the donation of oxo ligand through the trans influence.[43] The smaller shifts, 12 cm^{-1} for **5** and -24 cm^{-1} for **6**, are attributed to weak NH···S hydrogen bonds at the cis position. The lower-frequency shifts of ν(NH) in the W^{IV}O complexes are almost the same as those (-36 and -52 cm^{-1}, respectively) of the Mo^{IV}O complexes, $(NEt_4)_2[Mo^{IV}O\{1,2\text{-}S_2\text{-}3,6\text{-}(RCONH)_2C_6H_2\}_2]$ (R = CH$_3$, *t*-Bu).[31]

IR and Raman ν(W=O) bands of **3**−**7**, $(NEt_4)_2[W^{VI}O_2(bdt)_2]$ (**8b**),[43] and the related compounds[10,19] are summarized in Table 4. The W=O stretches of **3** and **4** were found at higher-frequency compared to **7** as $(NEt_4)_2[W^{IV}O\{1,2\text{-}S_2C_2(CN)_2\}_2]$ with electron-withdrawing groups.[10] A similar trend was found in the molybdenum analogues, where the corresponding ν(Mo=O) values for **3**, **4**, and **7** are 922, 924, and 905 cm^{-1}, respectively.[31] In the case of the dioxomolyndenum complexes, the W=O stretches of **5** and **6** are also higher-frequency shifted than those of **8b**. Such a large ν_s(W=O) value was observed for $(NEt_4)_2[W^{VI}O_2\{1,2\text{-}S_2C_2(CN)_2\}_2]$.[10] It is considered that electron-withdrawing CN groups weaken the W−S bond and compensatively strengthen the W=O bond through the trans influence. When an NH···S hydrogen bond is formed, the donation from S to W should be diminished. By the trans influence, π-donation of the oxygen atom should increase. Consequently, the strong W=O bonds were observed as higher-wavenumber shifts of ν(W=O) in the Raman and IR spectra; however, a significant shortening of the W=O bond was not found in the crystal structure of **5**·MeOH.

Table 5. UV−vis Absorption Maxima in DMF

	λ (nm) (ϵ, (M^{-1}cm^{-1}))		
W^{IV}O			
3	329 (9860)	398 (2790)	448 (1640)
4	336 (7990)	374 (3060)	444 (1330)
7[a]	325 (9000)	399 (1100)	423 (570)
W^{VI}O$_2$			
5	323 (16120)	425 (2540)	487 (1000)
6	342 (11100)	385 (7750)	525 (2190)
8b[a]	323 (15000)	419 (2300)	483 (1300)

[a] Ref 40.

Table 6. Redox Potentials in DMF

	E_{pa} (V)	E_{pc} (V)	$E_{1/2}$ (V)	$\Delta E_{1/2}$ (V)[b]
W^{IV}O				
3	−0.37	−0.31	−0.34	+0.29
4	−0.40	−0.30	−0.35	+0.28
7[a]			−0.63	
W^{VI}O$_2$				
5	−0.82	*c*		
6	−0.75	−0.60	−0.68	
8b[a]	−1.26	*c*		

[a] Ref 40. [b] Shifts from the redox potential of $(NEt_4)_2[W^{IV}O(bdt)_2]$ (**7**). [c] Not found.

UV Spectra and Raman Excitation Profile. The absorption maxima of **3**−**6** and the related compounds are summarized in Table 5. The spectrum of **3** shows the LMCT band at 329 and 398 nm, similar to **7**.[43] The spectrum of **5** is similar to that of **8b**.[43] Complexes **4** and **6** show similar

(43) Oku, H.; Ueyama, N.; Nakamura, A. *Bull. Chem. Soc. Jpn.* **1996**, *69*, 3139−3150.

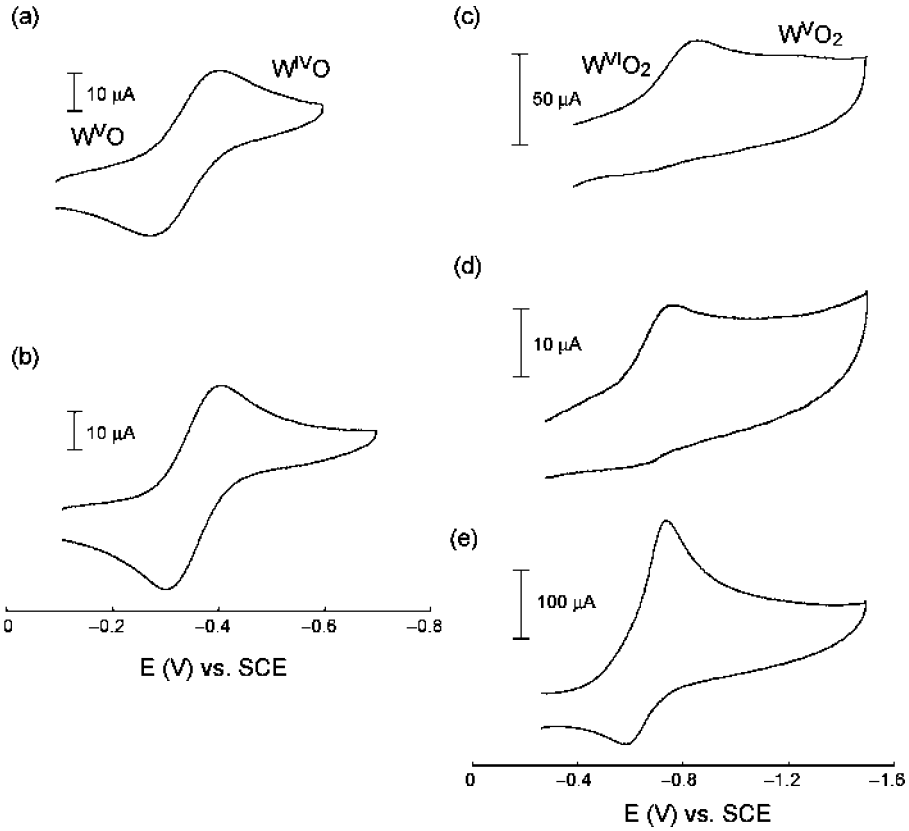

Figure 5. Cyclicvoltammograms of (a) **3** (0.1 v s^{-1}), (b) **4** (0.1 v s^{-1}), (c) **5** (0.5 v s^{-1}), (d) **6** (0.1 v s^{-1}), and (e) **6** (0.5 v s^{-1}).

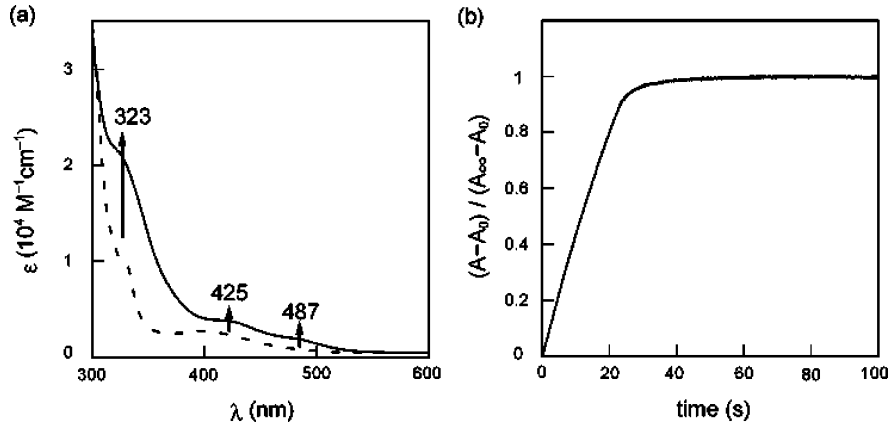

Figure 6. (a) Spectral changes in the reaction between **3** and Me_3NO in DMF at 27 °C with $[\mathbf{3}]_0 = 0.1$ mM and $[Me_3NO]_0 = 0.2$ mM. The dashed line was recorded before the reaction. The solid line was recorded after the reaction. (b) Time dependence of reduction monitored by absorption maximum at 323 nm for the kinetic analysis.

spectral patterns to **7** and **8b**, respectively, although showing the shifts of the absorption maxima from **7** and **8b**.

For **5**, the excitation profiles of the W═O stretching are shown in Figure 4. The enhancement of the resonance Raman vibrations are normalized to the peak intensity of 483 cm^{-1} for NEt_4^+. In the excitation profiles of $\nu_s(W^{VI}{=}O)$ and $\nu_{as}(W^{VI}{=}O)$ bands, the maximum was observed at 514.5 nm and the relative intensity ratios, $I/I_{483\ cm^{-1}}$, are 12.8 and 2.7, respectively. These profiles are similar to those of **8**, where the absorption bands in the range of 480−530 nm are attributed to the LMCT bands.[9]

Electrochemical Properties. The results of cyclic voltammetric studies are summarized in Table 6, and representative examples are shown in Figure 5. The reversible redox potentials of **3** and **4** are positively shifted by +0.28 to +0.29 V compared to −0.63 V of **7**. Such positive shifts in the $W^{IV}O$ complexes are similar to those (+0.25 and +0.36 V, respectively) of the corresponding $Mo^{IV}O$ complexes, $(NEt_4)_2[Mo^{IV}O\{1,2\text{-}S_2\text{-}3,6\text{-}(RCONH)_2C_6H_2\}_2]$ (R = CH_3, *t*-Bu).

The redox potentials of the dioxotungsten complexes with the 1,2-dithiolate ligand are known to be irreversible because of the instability of the W^VO_2 species generated.[43] The reduction potentials of **5** and **6** are positively shifted by +0.44 and +0.51 V, respectively, compared to −1.26 V of **8b**. In the repeated scans of **5** or **6**, the W(IV/V) redox current of **3** or **4** was gradually increased. This fact indicates the decomposition of the W^VO_2 species to monooxotungsten. As shown in Figure 5, when the scan rate increased to 0.5 V

s^{-1} from 0.1 V s^{-1}, an oxidation peak associated with W(V)−W(VI) conversion appeared for **6** but not for **5**. The bulky *t*-Bu groups presumably hinder the intermolecular reaction between reactive $W^{V}O_2$ species and the other reducing species.

Reaction. The oxidation of **3** and **4** by Me_3NO was monitored using UV−vis spectrophotometry. In the previous papers,[31,40] we used the following conditions: [Mo] = [W] = 1 mM and [Me_3NO] = 1, 2, or 10 mM. The oxidation of **3** by Me_3NO was too fast to monitor the spectral change accurately. Thus, a diluted solution (0.1 mM) was used. The time course of the UV−vis spectra for the reaction between **3** (0.1 mM) and Me_3NO(0.2 mM) is shown in Figure 6. The second-order rate constant (k_2) of **3**, until 50% conversion, was 4.4×10^2 M^{-1} s^{-1}, about 90 times larger than that (5 M^{-1} s^{-1}) of $[W^{IV}O(bdt)_2]^{2-}$.[43] The acceleration by the NH···S hydrogen bond is more remarkable in this case than the molybdenum complexes.[31] In the same conditions, except for the concentration, k_2 for the molybdenum analogue, $[Mo^{IV}O\{1,2\text{-}S_2\text{-}3,6\text{-}(CH_3CONH)_2C_6H_2\}_2]^{2-}$,[31] was 2.3 M^{-1} s^{-1}. The ease of oxidation of $W^{IV}O$ complex is a result of the more negative redox potential (−0.37 V) compared to that (−0.13 V) of the $Mo^{IV}O$ complex.[20] Such a metal effect on the oxo-transfer reaction was also observed in other $Mo^{IV}O$ and $W^{IV}O$ dithiolene complexes.[33] On the other hand, the k_2 value of **4** was 2.0 M^{-1} s^{-1}. The retardation of reaction rate by bulky substituents was also reported for $[Mo^{IV}O\{1,2\text{-}S_2\text{-}3,6\text{-}(t\text{-}BuCONH)_2C_6H_2\}_2]^{2-}$[31] and $[Mo^{IV}O(1,2\text{-}S_2\text{-}3\text{-}Ph_3SiC_6H_3)_2]^{2-}$.[44]

The reactions between **5** and triphenylphospine or benzoin ([**5**]/[substrate] = 1:10) were recorded using an NMR spectrometer. Compound **5** quantitatively converted to **3** by triphenylphosphine without the detection of intermediates. The observed pseudo-first-order rate constant (k_{obs}) was 1.9×10^{-6} s^{-1}. No reaction between **5** and benzoin proceeded, in contrast to the k_{obs} (9.5×10^{-6} s^{-1}) of **8b**. The W(VI) complexes with NH···S hydrogen bonds exhibit lower oxidation reactivities. The high-frequency-shifted W═O Raman bands of **5** support the deactivation of oxo ligand. This restrained oxidation is consistent with the acceleration of reduction of Me_3NO by **3** and **4**. The NH···S hydrogen bond stabilizes the $W^{VI}O_2$ moiety via the trans influence. The kinetics studies are not the most sophisticated possible, but they do support the hypothesis of hydrogen-bond stabilization of the oxo groups.

Conclusions

The NH···S hydrogen bond in dioxotungsten(VI) 1,2-benzenedithiolate complexes stabilizes the oxo ligand and restrains oxo transfer reactivity. In contrast, the NH···S hydrogen bonds in the monooxotungsten(IV) 1,2-benzenedithiolate complexes accelerate O-atom transfer reactions. In the active center of native tungsten enzyme or molybdenum enzyme, the catalytic reaction is presumably controlled by switching on and off of the NH···S hydrogen bond. When the NH···S hydrogen bond is broken, the oxo ligand is activated and will oxidize substrates to afford W(IV) species. In the reduced state, when the NH···S hydrogen bonds are formed, the reduction of substrate starts. On and off of the NH···S hydrogen bond would be controlled by the amino proton of N5 (Figure 1). The existence of the amino proton is further controlled by oxidation−reduction or ring-opening/closing of pyranopterin.[45−47] The oxidation states of metal center and pyranopterin moiety are probably associated each other to achieve an efficient catalytic cycle. It should be noted that this hypothesis is speculative at this stage but presents an approach to the solution to the mechanism of the regulation of the reactivity in tungsten and molybdenum enzymes.

Acknowledgment. This work was supported by the Grant-in-Aid from the Ministry of Education, Culture, Sports, Science, and Technology, Japan.

Supporting Information Available: X-ray crystallographic files in CIF format. This material is available free of charge via the Internet at http://pubs.acs.org.

IC060719T

(44) Oku, H.; Ueyama, N.; Kondo, M.; Nakamura, A. *Inorg. Chem.* **1994**, *33*, 209−216.

(45) McNamara, J. P.; Joule, J. A.; Hillier, I. M.; Garner, C. D. *Chem. Commun.* **2005**, 177−179.

(46) Enemark, I. M.; Garner, C. D. *J. Bioinorg. Chem.* **1997**, *2*, 817−822.

(47) Wei, C. C.; Crane, B. R.; Stuehr, D. J. *Chem. Rev.* **2003**, *103*, 2365−2383.